Analytical and Simulation Availability Models of ROADM Architectures

Matija Džanko[*], Branko Mikac[*], Vedran Miletić[‡], Norberto Amaya Gonzalez[†], Georgios S. Zervas[†] and Dimitra Simeonidou[†]

[*] University of Zagreb, Faculty of Electrical Engineering and Computing, Zagreb, Croatia,
Email: matija.dzanko@fer.hr, branko.mikac@fer.hr

[‡] University of Rijeka, Department of Informatics, Rijeka, Croatia
Email: vmiletic@inf.uniri.hr

[†] University of Bristol, Faculty of Engineering, Bristol, UK
Email: norberto.amaya@bristol.ac.uk, georgios.zervas@bristol.ac.uk, dimitra.simeonidou@bristol.ac.uk

***Abstract* –The paper presents analytical and simulation availability models for evaluation of optical node availability. Analytical models are developed for six ROADM (reconfigurable optical add and drop multiplexers) architectures. Availability / cost figures are calculated, compared and discussed. For one of ROADMs simulation model is created and Monte Carlo simulation of times to failure and times to repair is carried out. A new measure *k-out-of-n availability* of a node is introduced. Analytical and simulation availability figures are compared. The possibility of simulation model application to other node architectures is discussed.**

Keywords – ROADM; optical node architectures; analytical availability model; simulation availability model; Monte Carlo simulation; k-out-of-n availability.

I. INTRODUCTION

Transparent optical networks based on wavelength division multiplexing (WDM) are key enabling technology for efficient high-speed data transmission [1]. In such networks traffic is carried over all-optical connections, referred to as optical lightpaths. One lightpath represents one wavelength channel and its corresponding path across the network. Each lightpath starts at the E/O transmitter (ingress node), where the signal is *added*. When traversing the network towards its destination, the signal is switched all-optically at intermediate nodes. At the O/E receiver, the signal is *dropped* and converted to the electrical domain. The implementations of all-optical add, drop, and pass-through functions often require the use of optical add/drop multiplexers (OADMs). Initial versions of OADMs consisted of hard-wired optical components, where each change in node configuration required manual intervention. Due to the growing variety of applications and a need for supporting traffic dynamicity, reconfigurable optical add/drop multiplexers (ROADMs) have been introduced [2-4]. In ROADMs, optical switching functionalities are implemented by optical components that are controlled by well-defined control and management planes. Hence, lightpath reconfigurations can be done without technician intervention.

When considering ROADMs, an important issue is the number of switching degrees, i.e. the number of independent switching directions that can be supported. Each degree is often associated with the transmission fibre that connects the node with one of its neighbours. Early ROADMs had only two degrees and were used in bidirectional rings. Second generation ROADMs introduced a multi-degree capability for constructing mesh topologies. Although the number of degrees was increased, the problem of limited flexibility was still present. The possibilities to change the outgoing direction of an added lightpath, to change the incoming direction of a dropped lightpath or to change the transmission wavelength of the lightpath have not been deployed. Next generation ROADMs are addressing this lack of flexibility, aiming at the so-called *colourless*, *directionless* and *contentionless* features.

ROADM is colourless if wavelengths can be configured by the control software without port restrictions, i.e. wavelengths are not associated with any physical add/drop port of the ROADM. For example, each wavelength can be assigned to a lightpath independently to the source in the add/drop port. This function can be done by a tuneable transmitter.

ROADM is directionless if any add/drop function can be accomplished to/from any output/input fibre. Some node architectures restrict arbitrary wavelength usage in the add/drop section.

Colourless and directionless networks are not completely flexible. The main problem is that wavelength blocking can occur when two wavelengths of the same colour converge at the same add/drop structure at the same time, causing network contention. Contentionless ROADM removes wavelength contention from the add/drop portion of the ROADM so that a transmitter can be assigned to any wavelength as long as the number of signals with the same wavelength is not greater than the number of degrees of the ROADM. Therefore, ROADM is contentionless if it allows multiple copies of the

same wavelength to be added/dropped on a single add/drop module.

This paper is focused on the availability evaluation of colourless, directionless and contentionless (CDC) ROADMs [5, 6]. Six major node CDC ROADM architectures are introduced and compared in terms of availability and cost. The rest of the paper is organized as follows: Section II explains the selection of the component failure rates used in the availability and cost analysis. Section III describes ROADM architectures. Section IV reports on the results of availability analysis. Simulation model is introduced and Monte Carlo simulation is applied. Conclusions are drawn in Section V.

II. ROADM Component Failure Rate

The availability $A(t)$ of an optical component (system) is the probability that the component (system) works correctly in the time of observation t [7]. Usually unavailability $U(t)$ is used as complementary measure to $A(t)$, where $U(t)=1-A(t)$.

Assuming component failure rates λ and repair rates μ are constant, the mean time to failure *MTTF*, the mean time to repair *MTTR* and steady-state availability A can be calculated as follows:

$$MTTF=\frac{1}{\lambda} \qquad MTTR=\frac{1}{\mu} \qquad A=\frac{\mu}{\lambda+\mu} \tag{1}$$

The failure rates λ in the Table I and the component costs in Table II rely on data from several sources [8-12]. The component relative cost come from personal communication with vendors and researchers in the area. Component prices can vary, but assuming that the same relative prices are used in all architectures, the ratio of the total price between different architectures would stay the same. Failure rates are presented in FIT (number of failures in 10^9 hours). In addition to the component failure rate table, for each component it is noted where failure rate data were taken from.

TABLE I
COMPONENT FAILURE RATES

Component	Symbol	Failure rate [FIT]
Multiplexer / Demultiplexer	MUX/DEMUX	W×25
MEMS mirror	MIR	21
Splitter 1:N	SPL	N×25
Coupler N:1	CPL	N×25
Wavelength selective switch	WSS	N×250
Tuneable transponder	RX	470
Tuneable transmitter	TX	745
Tuneable filter	FIL	400

TABLE II
COMPONENT COSTS

Component	Symbol	Relative cost
Multiplexer / Demultiplexer	MUX/DEMUX	0.365
320 × 320 MEMS switch	OXC	23
8 × 8 MEMS connections	CON	5
Splitter 1:N	SPL	0.015
Coupler N:1	CPL	0.015
Wavelength selective switch 1:N	WSS	7.5 + 0.5×N
Tuneable transponder	RX	1
Tuneable transmitter	TX	1
Tuneable filter	FIL	0.015

Unit price (in this case relative cost is 1) is $3,500. In Table I and Table II, N represents the number of incoming/outgoing fibres and W the number of wavelengths per fibre. Failure rates of node components were estimated using the following assumptions:

Tuneable filter

The failure rate was obtained from [8].

MUX/DEMUX

The failure rate is proportional to the number of wavelengths per fibre. The basic value is 25 FIT per wavelength and the figure originates in [9], where failure rate is 100 FIT for 4 wavelengths, and 200 FIT for 8 wavelengths.

MEMS mirror

The failure rate was obtained from [10]. Static availability has been experimentally verified for more than two years over 4,000 switch elements. This leads to a verified estimate: λ is equal to 21 FIT.

Splitter 1:*N* / Coupler *N*:1

1:N power splitter where N is the number of incoming fibres. The elementary value was taken from [11], where failure rate is 50 FIT for 1:2 splitter.

Tuneable transmitter/receiver

Failure rate was obtained from [11].

WSS

Wavelength selective switch failure rate was taken from [12].

With described failure rates, we calculated the *MTTF* and A for each component used of the architecture. We estimate *MTTR* = 6 hours according to the repair data from the field. We assume the following: the number of wavelengths per fibre is 32, mux/demux have 32 input/output ports, and 2 input/output ports for add/drop function. 3D-MEMS is assumed to be switching device with 320 × 320 ports.

III. CDC ROADM Node Architecture

Several optical components are used for ROADM functional design [13]. Even though there are different ROADM implementations, the basic building blocks are the same. Fig. 1 show typical optical components used in ROADMs.

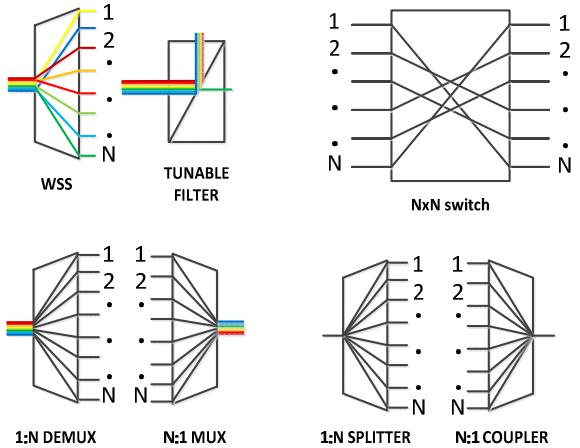

Fig. 1. Basic ROADM optical components

Optical splitters distribute optical signals from one input port to all output ports. When a splitter is used in the opposite direction, it becomes an optical coupler.

Multiplexer and demultiplexer are devices that couple or separate optical channels with different wavelengths.

A 1×N wavelength selective switch (WSS) is a device that switches selected wavelength(s) from an input port to any output port. The most common technologies used for WSS implementation are based on liquid crystal on silicon (LCoS) [14] and micro-electro-mechanical systems (MEMS) [15].

The optical switch provides all-optical signal switching without signal conversion to the electrical domain. For example, a 320 × 320 switch can provide a flexible add/drop ROADM structure.

For description of ROADM architectures, a set of parameters need to be defined:

- Node degree N
- Number of channels per fibre W
- Maximum number of add/drop channels L

We assume that all input and output ports are symmetric and all connections are bidirectional.

A. *First architecture:* ***DEMUXs + OXC + MUXs***

This architecture uses demultiplexers, OXC and multiplexers for achieving the CDC function [16]. Firstly, all DWDM channels from N input ports are demultiplexed into $N \times W$ channels. These channels, in conjunction with added channels (up to $L \times N$), are sent to a large optical cross-connect (with dimension $[(L + W) \times N) \times (L + W) \times N)]$). At the output end, the signals for each output port are combined through multiplexer. Dropped channels are sent to the tuneable transponders. The total number of transponders is $L \times N$. This architecture contains CDC features because optical cross-connect can switch any input fibre to any output fibre and each channel can be switched to any output port or dropped to any transponder. The disadvantage of this architecture is the requirement for a large scale OXC, which is expensive and can represent a single point of failure. In this paper it is assumed that the OXC control plane is highly redundant and only mirrors within the OXC matrix can fail. This architecture is depicted in Fig. 2.

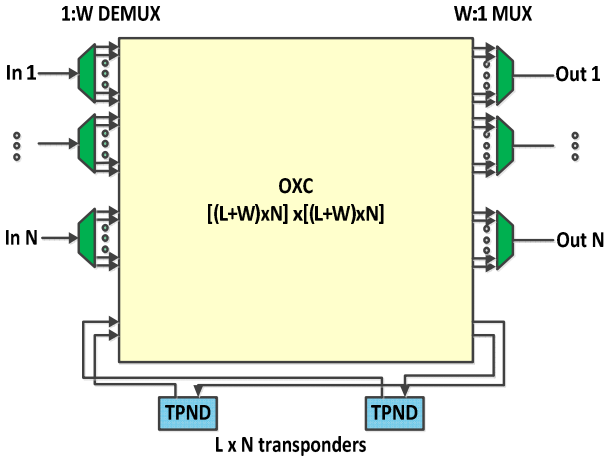

Fig. 2. The first architecture

The availabilities of pass-through, add and drop functions are given by multiplication of component availabilities that are used in each function:

$$A_{PASS} = A_{DEMUX}^{N} \cdot A_{MIR}^{2N(W-L)} \cdot A_{MUX}^{N}$$
$$A_{DROP} = A_{DEMUX}^{N} \cdot A_{MIR}^{2LN} \cdot A_{RX}^{N} \quad (2)$$
$$A_{ADD} = A_{TX}^{LN} \cdot A_{MIR}^{2LN} \cdot A_{MUX}^{N}$$

B. *Second architecture:* ***Splitter + WSS*** *+ tuneable filter array*

The difference among architectures 2-6 is in design of the add/drop module. The main components in the second architecture are splitters and WSSs. In this architecture, at each input port, the DWDM signal is split into N groups, among which N-1 groups are sent to other N-1 degree output ports. Dropped signals are switched to a colourless transponder through a transponder aggregator and achieve colourless function.

The drop function is implemented by the use of splitters, switches and optical filters. Firstly, dropped signals from each input port are sent to 1:($L \times N$) splitter. Afterwards, these signals are sent to an array of $L \times N$ units of selector, which consists of $N \times 1$ optical switch followed by a tuneable filter. In this case each of the $N \times 1$ optical switches can receive all input signals from all input ports. Tuneable filter selects particular channel of the DWDM signal which will be received by tuneable transponder.

The add function is realized by 1 × N switch, 1: ($L \times N$) coupler and WSS which selects outgoing wavelengths on output ports. Directionless operation is realized by switching added signals to respective output ports. WSS devices on each output port are used to select output signals and to avoid wavelength contention.

The disadvantages of this architecture are in high optical power loss due to the high port count splitters and high cost due to the large number of optical switches and tuneable filters. On Fig. 3 second architecture is shown.

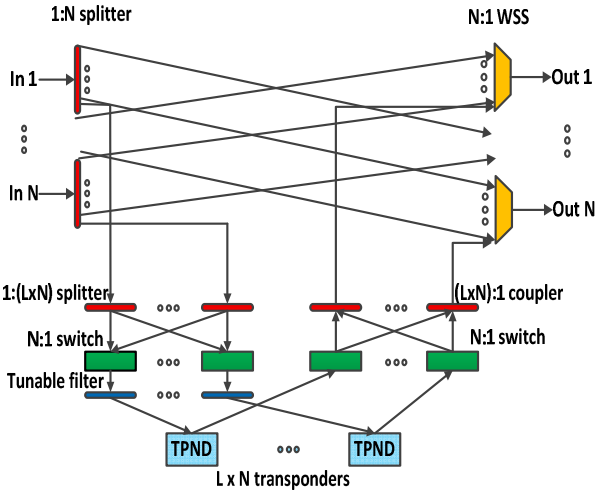

Fig. 3. The second architecture

Availability of pass-through, add and drop functions are given by:

$$A_{PASS} = A_{SPL}^{N} \cdot A_{WSS}^{N}$$
$$A_{DROP} = A_{SPL}^{N} \cdot A_{SPL}^{N} \cdot A_{SWITCH}^{LN} \cdot A_{FIL}^{LN} \cdot A_{RX}^{LN} \quad (3)$$
$$A_{ADD} = A_{TX}^{LN} \cdot A_{SWITCH}^{LN} \cdot A_{CPL}^{N} \cdot A_{WSS}^{N}$$

C. *Third architecture:* ***Splitter + WSS*** *+ DEMUX + OXC*

Pass-through function is implemented as in architecture 2: by splitters on each input fibre that sends N-1 copies of signal to N-1 degree output ports. Add/drop module is constructed using N units of 1:W demultiplexers and a $(N \times W) \times (N \times L)$ OXCs. Each demultiplexer separates the wavelengths, which are then sent to their respective transponders by arbitrary switching in the OXC. Some of the channels are directly cross-connected from ROADM inputs to outputs as they do not need to be dropped. That is the reason why the OXC has a higher number of input ports than the number of output ports ($N \times W > N \times L$). Third architecture is depicted in Fig. 4.

The availabilities of the pass-through drop and add functions are represented by:

$$A_{PASS} = A_{SPL}^{N} \cdot A_{WSS}^{N}$$
$$A_{DROP} = A_{SPL}^{N} \cdot A_{DEMUX}^{N} \cdot A_{MIR}^{NW} \cdot A_{MIR}^{LN} \cdot A_{RX}^{LN} \quad (4)$$
$$A_{ADD} = A_{TX}^{LN} \cdot A_{MIR}^{NW} \cdot A_{MIR}^{LN} \cdot A_{MUX}^{N} \cdot A_{WSS}^{N}$$

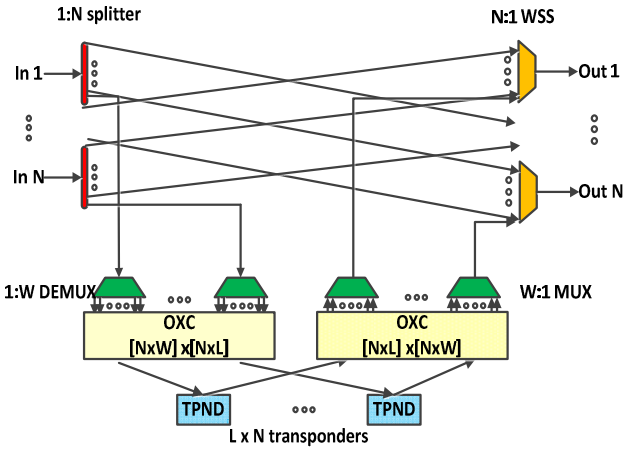

Fig. 4. The third architecture

D. *Fourth architecture:* ***Splitter + WSS*** *+ WSS + OXC*

Fig. 5 shows the fourth architecture. Pass-through switching is achieved by splitters in conjunction with WSSs. A combination of splitters and WSSs are used to implement the drop function. Splitters replicate the signal onto multiple standard WSS units. The WSSs select the channels that will be dropped and send them to a $(N \times L) \times (N \times L)$ OXC. The outputs of the OXC are connected to transponders. In the add module, another OXC is used in conjunction with N units of L:1 couplers to combine added signals.

The use of WSSs has the advantage of decreasing insertion loss but it is very expensive.

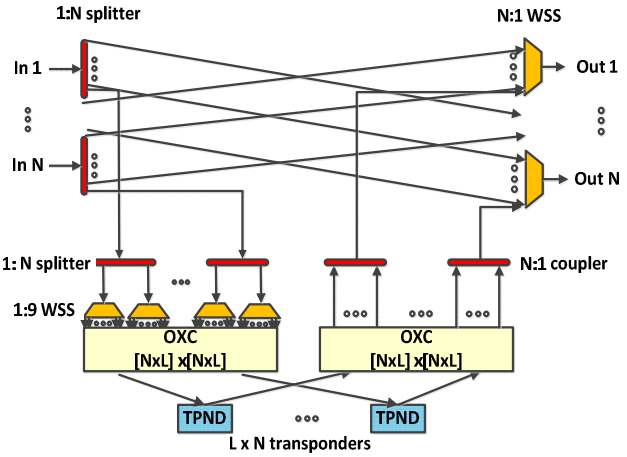

Fig. 5. The fourth architecture

Analytical formulas for availability of this architecture follow:

$$A_{PASS} = A_{SPL}^{N} \cdot A_{WSS}^{N}$$
$$A_{DROP} = A_{SPL}^{N} \cdot A_{SPL}^{N} \cdot A_{WSS}^{NK} \cdot A_{MIR}^{18NK} \cdot A_{RX}^{LN} \quad (5)$$
$$A_{ADD} = A_{TX}^{LN} \cdot A_{MIR}^{LN} \cdot A_{MIR}^{LN} \cdot A_{CPL}^{N} \cdot A_{WSS}^{N}$$

E. *Fifth architecture:* ***Splitter + WSS*** *+ HPC OXC + WSS*

The fifth architecture, shown in Fig. 6, is very similar to architecture 4, but instead of having cascaded couplers with WSSs in the add/drop module, high port count (HPC) WSSs are used.

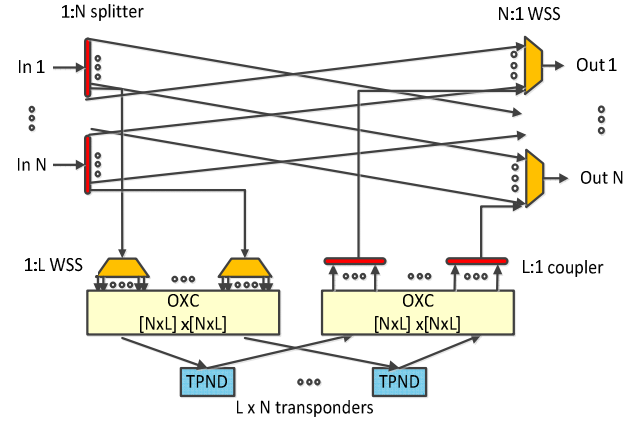

Fig. 6. The fifth architecture

Availabilities of pass-through, add and drop functions are given by formulas:

$$A_{PASS} = A_{SPL}^{N} \cdot A_{WSS}^{N}$$
$$A_{DROP} = A_{SPL}^{N} \cdot A_{WSS}^{N} \cdot A_{MIR}^{LN} \cdot A_{MIR}^{LN} \cdot A_{RX}^{LN} \quad (6)$$
$$A_{ADD} = A_{TX}^{LN} \cdot A_{MIR}^{LN} \cdot A_{MIR}^{LN} \cdot A_{CPL}^{N} \cdot A_{WSS}^{N}$$

F. *Sixth architecture:* ***WSS + coupler*** *+ OXC + coupler*

This architecture has WSSs connected to input ports, and couplers on output ports. In the drop module an OXC is used, while the add module is the same as in the fourth architecture, as illustrated in Fig. 7.

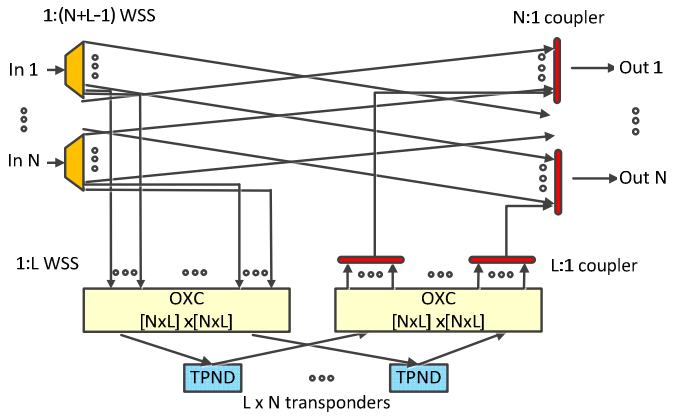

Fig. 7. The sixth architecture

Availabilities of three main functions are given by:

$$A_{PASS} = A_{WSS}^{N} \cdot A_{CPL}^{N}$$
$$A_{DROP} = A_{WSS}^{N} \cdot A_{MIR}^{LN} \cdot A_{MIR}^{LN} \cdot A_{RX}^{LN} \quad (7)$$
$$A_{ADD} = A_{TX}^{LN} \cdot A_{MIR}^{LN} \cdot A_{MIR}^{LN} \cdot A_{CPL}^{N} \cdot A_{CPL}^{N}$$

IV. AVAILABILITY FIGURES

A. *Analytical results*

In this section, the pass-through, add and drop function availabilities of the six architectures are compared. The pass-through availability comparison is presented in Fig. 8.

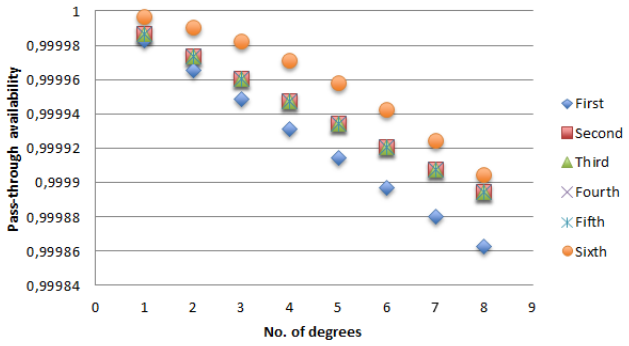

Fig. 8. Pass-through function availability

The sixth architecture has highest pass-through availability due to the fact that for small number of degrees small port count WSSs are used, while in architectures 2-5 WSSs port count doesn't change with the increase of input fibres. The first architecture has the lowest availability because one lightpath is passing through four elements (demultiplexer-mirror-mirror-multiplexer), while in the other architectures pass-through lightpath is consisted of two elements (WSS-splitter/coupler). The drop function availability comparison is shown on Fig. 9.

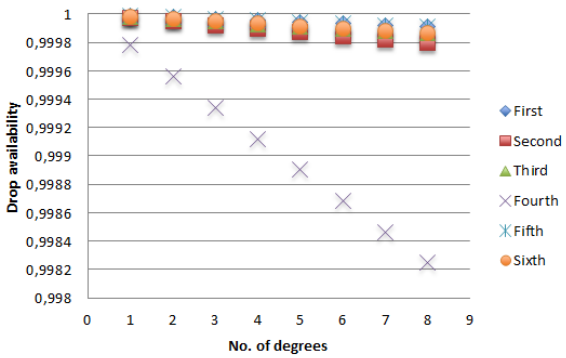

Fig. 9. Drop function availability

Drop availability is the lowest for the fourth architecture because the drop function has large number of components which have smaller availability than components used in drop functions in other architectures.

Fig. 10 presents the add availability comparison.

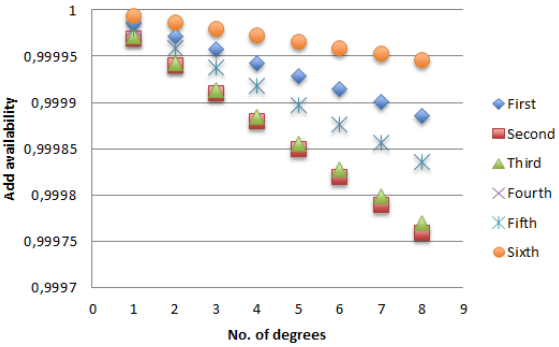

Fig. 10. Add function availability

Architectures 2 and 3 have the lowest add availability because they have the largest number of components in add module. When comparing cost (C) of six ROADM architectures, the fourth architecture has the highest price. The main reason for highest price in fourth architecture is the large number of expensive WSSs and OXCs in add and drop function. The cost comparison is shown in Fig. 11.

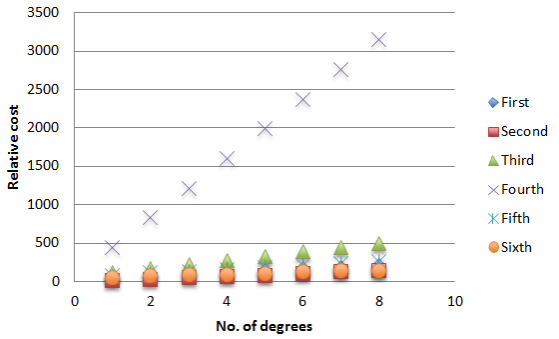

Fig. 11. Relative cost comparison

Efficiency E is defined as the ratio of availability (A) and cost (C), and it is depicted in Fig. 12.

$$E = \frac{A}{C} \quad (8)$$

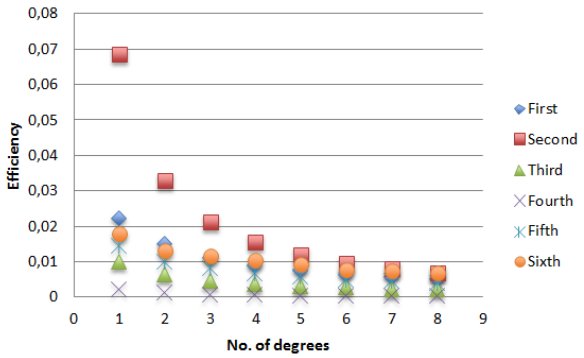

Fig. 12. Efficiency of ROADM architectures

Taking into account the efficiency of all six architectures, the second architecture is the best with the highest availability and cost ratio. First architecture has lower efficiency due to the fact that has expensive large port count OXC. If the OXC price would be near the price of WSS, the first architecture would have the highest efficiency.

B. Simulation results

In order to calculate availability performance for complex node structures, simulation models are developed. In this paper availability model for the first ROADM architecture is introduced and Monte Carlo simulation results are presented. The basic entity to be simulated is an optical component, which are connected in series, forming a lightpath. Lightpath represents a connection connecting one input and one output of the node. The set of lightpaths in the model is generated randomly for each simulation iteration. One iteration consists of a number of generated events referred to as failure or repair actions on photonic components.

An example depicted on Fig. 13 represents all randomly generated lightpaths passing through the first ROADM architecture (N=2, W=4 and L=1). Three types of lightpaths are considered: pass-through, add, and drop lightpaths. There are 10 lightpaths: 6-out-of-10 (blue ones) lightpaths belong to the pass-through type, 2-out-of-10 (green ones) belong to the add type and 2-out-of-10 (red ones) belong to the drop type.

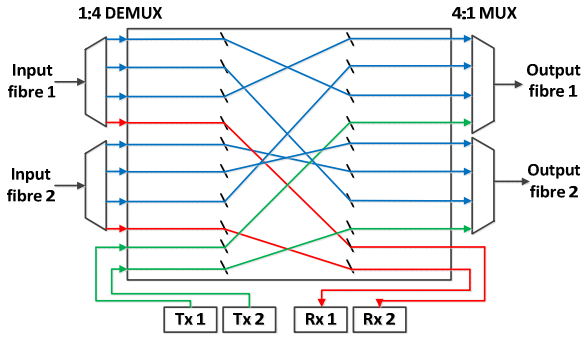

Fig. 13. An example of randomly generated set of lightpaths

When having all generated lightpaths within the architecture, it is possible to see how component failure/repair events relate to the availability of each lightpath or set of lightpaths.

Lightpath availability can be evaluated from the behaviour of the lightpath in time, where a lightpath alternates fault-free and faulty states. The lightpath availability is a function of photonic components' availabilities lightpath is passing through.

Availability model and simulation are based on the following assumption:

- Failure rate λ and repair rate μ are constant. As a consequence, probability density functions have exponential shape with parameters λ and μ, respectively. Constant failure rate λ relays to behaviour of components' failures during component operating period of life-cycle represented by "bath tub" curve.

Monte Carlo simulation is executed independently for each lightpath taking into account that a failure of a photonic component affecting more than one lightpath is simulated only once. The procedure is scheduled according to the following steps:

1. In time zero, all components are set to failure-free state.
2. Uniform distributed random number is generated in the interval [0,1).
3. Exponentially distributed time to failure (*TTF*) and time to repair (*TTR*), for each component in the architecture, are calculated according to the expressions:

$$TTF = \frac{-\ln(1-p)}{\lambda}, \quad TTR = \frac{-\ln(1-x)}{\mu} \tag{9}$$

where p and x are random numbers, generated in step 2, related to *TTF* and *TTR*, respectively.

4. Each lightpath is affected by the failures of the lightpaths' components creating their own lightpath timeline, alternating lightpath ON/OFF states. For each lightpath the cumulative *ONtime* and *OFFtime* are recorded. The availability of each lightpath can be calculated at the end of iteration by:

$$A = \frac{ONtime}{ONtime + OFFtime} \tag{10}$$

5. For each time interval between any two simulated events, the number of working lightpaths is enumerated. Achieved number k ($k \le n$, where n is the number of all lighpaths within the architecture) relays to the number of lightpaths which are in fault-free state in the interval. The measure *k-out-of-n-availability* is defined as the probability that at least k lightpaths are fault-free during entire simulated time. *K-out-of-n-availability* (on expression 11) is calculated as the ratio of time in which k or more than k lightpaths are in faulty-free state and the total simulation time.

$$k-out-of-n-A = \frac{time_{ONlightpaths>=k}}{TOTALtime} \tag{11}$$

N-out-of-n availability is depicted on the Fig. 14. The grey areas represent the intervals when all lightpaths in the node are fault-free (*n-out-of-n available*). In opposite, the white areas represent the intervals when at least one lightpath is in faulty state. Note, by using presented

model and Monte Carlo simulation it is possible to calculate *k-out-of-n-availability*.

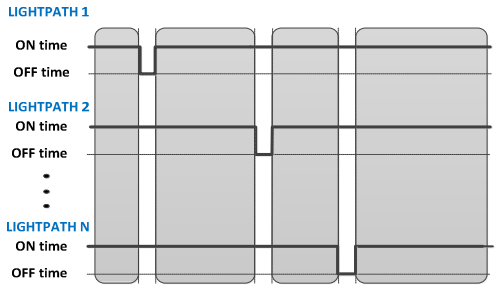

Fig. 14. Timelines of lightpaths

C. Comparison of analytical and simulation results

The availability comparison of analytical and simulation results for the first ROADM architecture (*N* varies from 2 to 8, *W*=32, and *L*=2) is depicted on Fig. 15. Availability figures compared are related to the *n-out-of-n availability* measure. The choice of the measure lies in the fact that early presented analytical formulas are derived for this case. Analytical formulas for other cases, where the numbers of working lightpaths are less than *n* are more complex. The differences between the analytical and simulation results are found to be in order of magnitude of 10^{-5} for total number of approximate 5000 simulated events. The deviation comes from the nature of simulation approach where the accuracy depends on the number of generated events. In case of a higher number of simulated event or longer period of simulated time more accurate results are achieved. Note, simulated real time is limited only by the requirement that Monte Carlo simulation has to run in reasonable CPU time. The "unlimited" simulated time is possible because failure and repair rates, λ and μ, are assumed to be invariant in time.

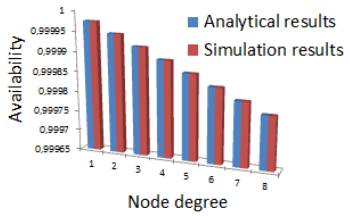

Fig. 15. The comparison of analytical and simulation results for the first ROADM architecture

As the analytical and simulation approaches in calculating availability produce comparable results, the assumption is that the simulation model could be applied to a variety of architectures, especially for the cases where availabilities cannot be calculated by means of the analytical approach.

V. Conclusion

The paper compares six ROADM architectures in terms of availability and cost. The failure rates of the optical components were taken or derived from the references. Based on the given component failure rates and assumed repair rates, the availabilities of pass-through, drop and add functions for each ROADM architecture were calculated.

Analytical formulas describe the availabilities of the presented node architectures. A novel simulation model for node availability evaluation is introduced. In addition, event-driven Monte Carlo simulation on the model is applied. Analytical and simulation results are found comparable for *n-out-of-n availability* model. In this way the possibility is opened for evaluation of general *k-out-of-n availability* models by using Monte Carlo failure simulation of complex node architectures in the cases where analytical approach cannot be used. The second ROADM architecture has been evaluated as the most cost-effective architecture with respect to the ratio of availability and cost. In the future research the simulation model will be extended to other perspective node architectures.

References

[1] S. Gringeri, et. al., "Flexible Architectures for Optical Transport Nodes and Networks", *IEEE Comm. Mag.*, July 2010, pp. 40-50, vol. 48, Iss. 7.

[2] K. Yu, et. al., "A Novel Broadband ROADM for Optical Network", *Proceedings of the 7th WICOM,*September 2011, China, pp.1-3.

[3] T. S. El Bawab, "ROADMs: Foundation for True Reconfigurable Optical Networking", *Proceedings of the GLOBECOM Workshops*, December 2008, pp.1-2.

[4] T. A. Strasser, J. Taylor, "ROADMs Unlock the Edge of the Network", *IEEE Communications Magazine*, July 2008, vol. 46., pp. 146-149.

[5] P. Roorda, B. Collings, "Evolution to Colorless and Directionless ROADM Architectures", *Proceedings of the OFC/NFOEC*, Feb. 2008., San Diego, USA, pp. 1-3.

[6] A. Devarajan, et al., "Colorless, Directionless and Contentionless multi-degree ROADM architecture for mesh optical networks", *Proceedings of the Communications Systems and Networks Conference,* 2010,Bangalore, India, pp.1-10.

[7] R. Inkret, M. Lackovic, B. Mikac, "WDM Network Availability Performance Analysis for the COST 266 Case Study Topologies", *Proceedings of the ONDM*, Budapest 2003, pp. 1201-1220.

[8] L. Wosinska, "Reliability study of fault-tolerant multiwavelength nonblocking optical cross connect based on ingaasp/inp laser-amplifier gate-switch arrays," *J. Lightwave Technology,* October 1993*,* vol. 5, no. 10, pp. 1206-1209.

[9] L. Wosinska and L. Thylen, "Reliability performance of optical cross-connect switches - requirements and practice" *in Proceedings of the OFC'98*, San Jose, USA, pp.28.-29.

[10] P. de Dobbelaere, K. Falta, and S. Gloekner,"Advances in integrated 2D MEMS-based solutions for optical network applications", *IEEE Commun. Mag*., May 2003, pp. s16-s23.

[11] L. Wosinska, L. Thylen, and R. P. Holmstrom, "Large capacity strictly nonblocking optical cross-connects based on microelectro-optomechanical (MEOMS) switch matrices: Reliability performance analysis," *J. Lightwave Technol.*, August 2011*,* vol. 19, pp. 1065-1075.

[12] A. Morea, I. B. Heard, "Availability of Translucent Networks Based on WSS Nodes, Comparison with Opaque Networks", *in Proceedings on ICTON*, UK, 2006., pp. 43 – 47.

[13] E.B. Basch, "Architectural Tradeoffs for Reconfigurable Dense Wavelength-Division Multiplexing Systems", *IEEE Journal of Selected Topics in Quantum Electronics*, July 2006, vol. 12., Iss. 4, pp. 615-626.

[14] G. Baxter et.al. "Highly programmable Wavelength Selective Switch based on Liquid Crystal on Silicon switching elements" in *Proceedings OFC/NFOEC* 2006, OTuF2, Anaheim, California, USA.

[15] S. de Hennin et.al. "Addressing Manufacturability and Reliability of MEMS-based WSS", *in Proceedings of the OFC/NFOEC* 2007, Ottawa, Canada, pp. 1-3

[16] S. Thiagarajan, "Direction-Independent Add/Drop Access for Multi-Degree ROADMs", *in Proceedings of the OFC/NFOEC 2008*., San Diego, pp.1-3.